Inorg. Chem. **2002**, *41*, 2839–2847

Catalytic Effect of Sulfoxides on the Fluxional Motion of 2,9-Dimethyl-1,10-phenanthroline in a Platinum(II) Complex: Evaluation of Steric and Electronic Contributions

Raffaello Romeo,* Lucia Fenech, Salvatore Carnabuci, Maria Rosaria Plutino, and Andrea Romeo

Dipartimento di Chimica Inorganica, Chimica Analitica e Chimica Fisica and ISMN, CNR, Sezione di Messina, Università di Messina, Salita Sperone 31, Villaggio S. Agata, 98166 Messina, Italy

Received November 27, 2001

Addition of external weak nucleophiles to a chloroform solution of the cationic complex ion [Pt(Me)(dmphen)(PPh_3)]$^+$ (**1**) accelerates the fluxional motion of the symmetric chelating ligand 2,9-dimethyl-1,10-phenanthroline (dmphen) between nonequivalent exchanging sites. The rates of the dynamic process can be measured by lineshape analysis of the ^{1}H NMR spectra. Concentration-dependent measurements were carried out with the ligands $SOMe_2$, $SO(CH_2)_4$, SO(*n*-Bu)$_2$, SO(*sec*-Bu)$_2$, SO(*i*-Pr)$_2$, SOEt(Ph), SOPr(Ph), SO(Bz)$_2$, SO(*p*-MeC_6H_4)$_2$, $SOPh_2$, SO(*p*-ClC_6H_4)$_2$, SOMe(*p*-$MeOC_6H_4$), SOMe(*p*-MeC_6H_4), SOMe(Ph), SOMe(*p*-BrC_6H_4), and SOMe(*p*-ClC_6H_4). The rate constants k_{obsd}, when plotted against the concentration of the added ligands SOR(R′), give a family of straight lines with a common intercept, indicating that the two-term rate law $k_{obsd} = k_1 + k_2$[SOR(R′)] is obeyed. The same rate law applies to the displacement of $SOMe_2$ from [Pt(Me)(phen)($SOMe_2$)]$^+$ (**2**) (phen = 1,10-phenanthroline) by sulfoxides ($SOMe_2$, SO(*i*-Pr)$_2$, SOMe(*p*-$MeOC_6H_4$), SO(*p*-MeC_6H_4)$_2$, $SOPh_2$, SO(*p*-ClC_6H_4)$_2$, and SO(*sec*-Bu)$_2$). The fluxional rates in **1** are 6–7 orders of magnitude higher than the substitution rates in **2**. The values of the rate constants for the two processes were resolved quantitatively into steric and electronic contributions by use of quantitative analysis of ligand effects (QALE). Inhibitory steric effects are linearly operative for the entire set of ligands, the rates of the reactions are enhanced with increasing electron donor capacity of the sulfoxides, and there is a small but significant E_{ar} effect that enhances the reactivity of the aryl sulfoxides. The strict similarity of the patterns of the two processes and of their dependence upon the stereoelectronic properties of the ligands, combined with the intrinsic lability of the platinum–nitrogen bonds, would suggest the operation of stereospecific consecutive ring-opening and ring-closure steps for the fluxional motion of dmphen in **1**. However, the available evidence does not allow alternative mechanisms involving intramolecular rearrangements of the five-coordinate intermediate to be ruled out.

Introduction

In a recent kinetic study[1] we showed that the dinitrogen ligand 2,9-dimethyl-1,10-phenanthroline (dmphen), in the monoalkyl cationic complex ion [Pt(Me)(dmphen)(PPh_3)]$^+$ (**1**), is characterized by a fast fluxional motion between two different exchanging sites. The X-ray structure of **1** showed severe steric distortions in the coordination geometry and in the phenanthroline ligand, as well as a significant elongation of the Pt−N1 (2.152(3) Å) and Pt−N2 (2.162(3) Å) bond separations, caused by the *trans* influence of the methyl and phosphine groups acting as strong σ donors. The interionic solution structure was investigated in $CDCl_3$ at low temperature by ^{1}H-NOESY and ^{19}F{^{1}H}-HOESY NMR spectroscopies, and the anions PF_6^- (**1a**) and BF_4^- (**1b**) showed strong contacts with the cation [Pt(Me)(dmphen)(PPh_3)]$^+$, being located preferentially on the side of the phenanthroline ligand and thus forming tight ion pairs.

The dynamic exchange process was studied by variable-temperature NMR spectroscopy, as a function of the nature of the counteranion, of the solvent, or of added nucleophiles.

* To whom correspondence should be addressed. Fax: ++39-090-393756. Phone: ++39-090-391984. E-mail: Raf.Romeo@chem.unime.it.

(1) Romeo, R.; Fenech, L.; Monsù Scolaro, L.; Albinati, A.; Macchioni, A.; Zuccaccia, C. *Inorg. Chem.* **2001**, *40*, 3293−3302.

10.1021/ic011206j CCC: $22.00
Published on Web 05/04/2002

The mechanism is switchable between dissociative and associative pathways, depending on the interionic structure of the complex and the action of potential nucleophiles. The first process is prevalent within the ion pair formed by a "noncoordinating" anion with the cationic complex and involves (i) initial dissociation of the metal−nitrogen bond, (ii) fast interconversion between two three-coordinate T-shaped intermediates containing η^1-coordinated dmphen, and (iii) final ring closure. The associative mechanism is promoted by addition of external ligands such as SO(*n*-Bu)$_2$, SO(*sec*-Bu)$_2$, and S(*sec*-Bu)$_2$, which have the effect of accelerating the fluxionality rate without inducing intermolecular exchange. We observed a significant nucleophilic discrimination ability among these ligands, as a result of differences in their electronic and steric properties. A variety of associative mechanisms can be envisaged for the accelerated flipping: (i) a sequence of nucleophilic substitution reactions which take place with retention of configuration or (ii) an intramolecular rearrangement from a five-coordinate intermediate, such as a Berry pseudorotation or a "turnstile" mechanism.[2] We were inclined to think that the first process was operative because of the correspondence observed between the catalytic efficiency of the ligands in promoting the fluxional motion and their nucleophilic power, even though the comparison could have been made only on a fairly low number of nucleophiles.

In this paper the dynamic exchange process of the dinitrogen ligand on complex **1** in $CDCl_3$ was investigated by NMR spectroscopy, as a function of the nature and the concentration of an extended series of sulfoxides of widely different electronic and steric properties. The application of QALE (quantitative analysis of ligand effects)[3] to the rate data provided a means of ascertaining the relative importance of the electronic and steric properties of the sulfoxide ligands in governing the fluxionality of the substrate. The way in which the size and the electron-releasing ability of the substituents on the sulfur atom influence the fluxionality of **1** was correlated with the effects observed in the bimolecular substitution reaction of $SOMe_2$ from $[Pt(Me)(phen)(SOMe_2)]^+$ (**2**) (phen = 1,10-phenanthroline) with a number of different sulfoxides. Although the mechanism for the fluxional motion of dmphen in complex **1** could not be determined unambiguously, the operation of a conventional consecutive displacement mechanism would most readily account for the pattern of behavior observed. This seems to be one of the first attempts to use QALE as a diagnostic tool in assessing the reaction mechanism.

Scheme 1. Wire Frame Schematization of the Molecular Structures of **1** and **2**

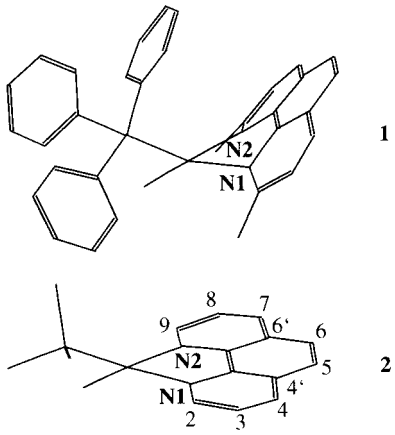

Results

The structural features of compounds **1** and **2** have been well established through X-ray diffraction studies.[1,4] The differences between the two complexes are significant (see Scheme 1) as far as the distortion of the phenanthroline ligand and the Pt−N separations are concerned. In the complex $[Pt(Me)(phen)(SOMe_2)]PF_6$[4] the 1,10-phenanthroline ligand is planar and coordinates to the Pt atom with a bite angle of 79.3(2)°; the Pt−N2 and Pt−N1 bond separations are significantly shorter than those of **1**, being 2.135(4) vs 2.162(3) Å and 2.075(4) vs 2.152(3) Å, respectively. The addition of external amounts of sulfoxides to **1** leads simply to an acceleration in the intrinsic fluxional rate of dmphen, while for **2** the only process observed is the substitution of the coordinated $SOMe_2$ by the entering nucleophile.

Dynamic Behavior of Complex 1. The above-mentioned dynamic process in the cationic $[Pt(Me)(dmphen)(PPh_3)]^+$ species was investigated in $CDCl_3$ as a function of the nature and of the concentration of the added ligands SOR(R′). At low temperature (260 K), the NMR spectrum of **1**, besides the resonances of the triphenylphosphine (δ in the range of 7.54−7.41 ppm) and of a methyl group directly coordinated to the metal (δ 0.73, $^2J_{PtH}$ = 66.9 Hz), shows two singlets, one for each methyl (at δ 3.08 and 1.95, respectively), four doublets, for H_3 (δ 7.90), H_8 (δ 7.29), H_4 (δ 8.64), and H_7 (δ 8.46) protons, and an AB system, for H_5 (δ 8.04) and H_6 (δ 8.01) protons, as a result of the asymmetry of a firmly bonded bidentate phenanthroline.

Figure 1 shows the changes in the ^{1}H NMR spectra of **1** upon the addition of increasing amounts of dmso-d_6. The

(2) (a) Ugi, I.; Marquarding, D.; Klusacek, H.; Gillespie, P. *Acc. Chem. Res.* **1971**, *4*, 288−296. (b) Casares, J. A.; Espinet, P. *Inorg. Chem.* **1997**, *36*, 5428−5431. (c) Stockland, R. A. Jr.; Anderson, G. K. *Organometallics* **1998**, *17*, 4694−4699.

(3) (a) Wilson, M. R.; Liu, H.-Y.; Prock, A.; Giering, W. P. *Organometallics* **1993**, *12*, 2044−2050. (b) Panek, J. S.; Prock, A.; Eriks, K.; Giering, W. P. *Organometallics* **1990**, *9*, 2175−2176. (c) Rahman, Md. M.; Liu, H.-Y.; Eriks, K.; Prock, A.; Giering, W. P. *Organometallics* **1989**, *8*, 1−7. (d) Rahman, Md. M.; Liu, H.-Y.; Prock, A.; Giering, W. P. *Organometallics* **1987**, *6*, 650−658. (e) Golovin, M. N.; Rahman, M. M.; Belmonte, J. E.; Giering, W. P. *Organometallics* **1985**, *4*, 1981−1991. (f) Eriks, K.; Giering, W. P.; Liu, H.-Y.; Prock, A. *Inorg. Chem.* **1989**, *28*, 1759−1763. (g) Tracey, A. A.; Eriks, K.; Prock, A.; Giering, W. P. *Organometallics* **1990**, *9*, 1399−1405. (h) Chen, L.; Poë, A. J. *Inorg. Chem.* **1989**, *28*, 3641−3647. (i) Brodie, N. M.; Chen, L.; Poë, A. J. *Int. J. Chem. Kinet.* **1988**, *20*, 467−491. (j) Poë, A. J. *Pure Appl. Chem.* **1988**, *60*, 1209−1216. (k) Dahlinger, K.; Falcone, F.; Poë, A. J. *Inorg. Chem.* **1986**, *25*, 2654−2658. (l) Farrar, D. H.; Hao, J.; Poë, A. J.; Stromnova, T. A. *Organometallics* **1997**, *16*, 2827−2832. (m) Hudson, R. H. E.; Poë, A. J. *Organometallics* **1995**, *14*, 3238−3248. (n) Farrar, D. H.; Poë, A. J.; Zheng, Y. *J. Am. Chem. Soc.* **1994**, *116*, 6252−6261. (o) Chen, L.; Poë, A. J. *Coord. Chem. Rev.* **1995**, *143*, 265−295. (p) Neubrand, A.; Poë, A. J.; van Eldik, R. *Organometallics* **1995**, *14*, 3249−3258.

(4) Bruno, G.; Nicolò, F.; Scopelliti, R.; Arena, G. *Acta Crystallogr., Sect. C: Cryst. Struct. Commun.* **1996**, *C52*, 827−829.

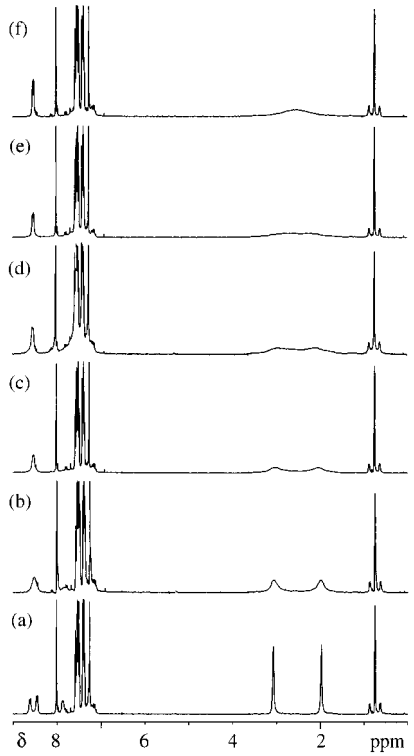

Figure 1. ^{1}H NMR spectra of compound **1** at 298 K in $CDCl_3$ as a function of dmso-d_6 concentration. Ligand concentrations ([dmso-d_6]/*m*) and rate constants (k_{obsd}/s^{-1}) for the fluxional motion of 2,9-dimethyl-1,10-phenanthroline in **1** are as follows: (a) [dmso-d_6] = 0, k_{obsd} = 19; (b) [dmso-d_6] = 0.00295, k_{obsd} = 158; (c) [dmso-d_6] = 0.00589, k_{obsd} = 316; (d) [dmso-d_6] = 0.00884, k_{obsd} = 484; (e) [dmso-d_6] = 0.0118, k_{obsd} = 633; (f) [dmso-d_6] = 0.0177, k_{obsd} = 967.

initial spectrum, in the lower plot of the figure, was recorded at 298 K in pure $CDCl_3$ and maintains much of the characteristics illustrated above for the spectrum taken at 260 K. On adding increasing amounts of dmso-d_6, the two methyls and the aromatic proton pairs H_3–H_8, H_4–H_7, and H_5–H_6 become chemically equivalent, indicating a fast site exchange of the two nitrogen atoms of the dmphen ligand.

The rate constant k_{obsd}, measured on the methyl signals, increased linearly with increasing concentration of dimethyl sulfoxide. Concentration-dependent measurements, carried out with the ligands $SO(CH_2)_4$, $SO(n\text{-}Bu)_2$, $SO(sec\text{-}Bu)_2$, $SO(i\text{-}Pr)_2$, SOEt(Ph), SOPr(Ph), $SO(Bz)_2$, $SO(p\text{-}MeC_6H_4)_2$, $SOPh_2$, $SO(p\text{-}ClC_6H_4)_2$, $SOMe(p\text{-}MeOC_6H_4)$, $SOMe(p\text{-}MeC_6H_4)$, SOMe(Ph), $SOMe(p\text{-}BrC_6H_4)$, and $SOMe(p\text{-}ClC_6H_4)$, exhibited a similar behavior. The rate constants k_{obsd} (see Supporting Information Table S1), when plotted against the concentration of the added ligands SOR(R′), give straight lines with a common intercept (Figure 2), indicating that the two-term rate law

$$k_{obsd} = k_1 + k_2[SOR(R')] \quad (1)$$

is obeyed. The values of k_2 (m^{-1} s^{-1}), from linear regression analysis of the dependence of k_{obsd} on [SOR(R′)], are listed in Table 1 as log k_2. The concentration-independent rate constant k_1 measures the rate of dmphen flipping within the ion pair $\{[Pt(Me)(dmphen)(PPh_3)]^+PF_6^-\}$,[1] while the second-order rate constant k_2 measures the efficiency of uncoordinated sulfoxides in accelerating the fluxionality.

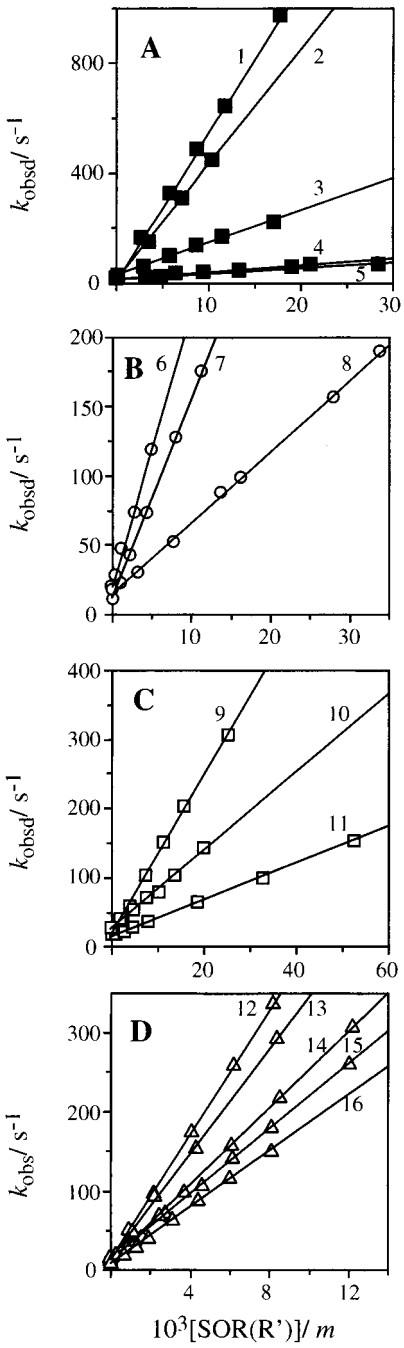

Figure 2. Dependence of the pseudo-first-order rate constants (k_{obsd}/s^{-1}) for the fluxional motion of dmphen in complex **1** upon sulfoxide concentration, at 298 K in $CDCl_3$. The numbers refer to the sulfoxides as listed in Table 1. Plot A is for the aliphatic SOR_2 sulfoxides, plot B the mixed sulfoxides, plot C $SO(p\text{-}XC_6H_4)_2$, and plot D $SOMe(p\text{-}XC_6H_4)$.

The rate constants for the flipping of complex **1** at different temperatures (in the range 242−311 K) and at a constant concentration of added dmso-d_6 of 8.66 m*m* were determined by line-shape analysis of the ^{1}H NMR spectra (Supporting Information Table S2 and Figure S1). The activation parameters for the catalyzed fluxional process were derived from the Eyring plot and are as follows: $\Delta H^{\ddagger} = 24.2 \pm 0.5$ kJ mol^{-1} and $\Delta S^{\ddagger} = -70 \pm 2$ J K^{-1} mol^{-1}.

Table 1. Selected Stereoelectronic Parameters of Sulfoxides **1**−**16**, Rate Constants for Their Catalytic Effect on the Fluxional Motion of the Dinitrogen Ligand 2,9-Dimethyl-1,10-phenanthroline in [Pt(Me)(PPh_3)(dmphen)]PF_6, and Rate Constants of $SOMe_2$ for SOR(R′) Substitution from [Pt(Me)(Me_2SO)(phen)]TFTB[a]

sulfoxide	$\sum\sigma^*$ [b]	χ[c]	θ[d]	θ[e]	E_{ar}[f]	log k_2[g]	log $k_{2'}$[h]
$SOMe_2$ (**1**)	0.00	5.70	79	111	0	4.731	−2.220
$SO(CH_2)_4$ (**2**)	−0.18			110		4.623	
SO(*n*-Bu)$_2$ (**3**)	−0.23	3.95	91	128	0	4.130[i]	
SO(*sec*-Bu)$_2$ (**4**)	−0.19	3.44	107	141	0	3.389[i]	−2.947
SO(*i*-Pr)$_2$ (**5**)	−0.38	2.30	107	141	0	3.339	−2.533
SOEt(Ph) (**6**)	0.50	6.52	92	130	1	4.167	
SOPr(Ph) (**7**)	0.48	6.22	92	130	1	4.293	
$SO(Bz)_2$ (**8**)	0.44					3.711	
SO(*p*-MeC_6H_4)$_2$ (**9**)	0.86	7.66	97	124	2	4.040	−2.695
$SOPh_2$ (**10**)	1.20	8.84	97	124	2	3.758	−2.991
SO(*p*-ClC_6H_4)$_2$ (**11**)	1.60	11.20	97	124	2	3.414	−3.910
SOMe(*p*-$MeOC_6H_4$) (**12**)	0.33	6.35	88	120	1	4.597	−2.428
SOMe(*p*-MeC_6H_4) (**13**)	0.43	6.68	88	120	1	4.522	
SOMe(Ph) (**14**)	0.60	7.30	88	120	1	4.392	
SOMe(*p*-BrC_6H_4) (**15**)	0.83			120		4.336	
SOMe(*p*-ClC_6H_4) (**16**)	0.83	8.45	88	120	1	4.252	

[a] At 298 K in $CDCl_3$. [b] Sum of the Taft σ^* constants for the radicals R and R′ bonded to sulfur in SOR(R′). [c] Fractional values calculated from the phosphorus(III) values (see ref 6); χ values (cm^{-1}) were taken from ref 5. [d] Fractional values calculated from phosphorus(III) values. θ values (deg) were taken from ref 5. [e] Values of circular cone apertures taken from ref 13. [f] Number of aryl rings bonded to the sulfur atom. [g] Logarithm form of second-order rate constants (m^{-1} s^{-1}) for the fluxional motion of dmphen in **1** under the accelerating effect of SOR(R′). [h] Logarithm form of second-order rate constants (m^{-1} s^{-1}) for the displacement of $SOMe_2$ from **2** by SOR(R′). [i] From ref 1.

Substitution Reactions. The reactions

$$[Pt(Me)(phen)(SOMe_2)]^+ + SOR(R') \rightarrow [Pt(Me)(phen)(SOR(R'))]^+ + SOMe_2 \quad (2)$$

($SOR(R') = SOMe_2$, SO(*sec*-Bu)$_2$, SO(*i*-Pr)$_2$, SO(*p*-MeC_6H_4)$_2$, $SOPh_2$, SO(*p*-ClC_6H_4)$_2$, and SOMe(*p*-$MeOC_6H_4$)) were carried out in $CDCl_3$ as solvent at 298 K. The analysis of the changes of the ^1H NMR spectra during the course of the reaction showed that the process under study was indeed the simple substitution of the bound $SOMe_2$ by SOR(R′). The systematic kinetics of this reaction were studied, under pseudo-first-order conditions, at different ligand concentrations and were followed by ^1H NMR spectroscopy. The changes in the intensity of the signals of bound and free $SOMe_2$ with time were used for the calculation of the rate constants. In some cases the reactions went to completion (with dmso-d_6, SO(*i*-Pr)$_2$, and SOMe(*p*-$MeOC_6H_4$) as entering groups), and the pseudo-first-order rate constants k_{obsd} (see Supporting Information Table S3), plotted against the concentration of the entering sulfoxide, gave straight lines with a zero intercept, indicating that in the two-term rate equation (1) the k_1 term makes little if any contribution to the reactivity (k_1 arises from the solvolytic path, and $k_{2'}$ is the second-order rate constant for the bimolecular attack of SOR(R′) on the substrate). The values of $k_{2'}$ were obtained from linear regression analysis of the rate law, and log $k_{2'}$ values are collected in Table 1, together with those of the other reagents calculated as discussed in the Experimental Section.

Discussion

The addition of external sulfoxide ligands to **1** in chloroform solution accelerates the fluxionality of dmphen without promoting any detectable exchange between free and coordinated ligands. The rates (log k_2, in Table 1) are 6−7 orders of magnitude greater than the rates of nucleophilic substitution of a ligand ($SOMe_2$) from the parent 1,10-phenanthroline complex **2** (log $k_{2'}$, in Table 1). The catalytic efficiency of the added ligands on the rearrangement decreases in the order $SOMe_2$ > $SO(CH_2)_4$ > SOMe(*p*-$MeOC_6H_4$) > SOMe(*p*-MeC_6H_4) > SOMe(Ph) > SOMe(*p*-BrC_6H_4) > SOPr(Ph) > SOMe(*p*-ClC_6H_4) > SOEt(Ph) > SO(*n*-Bu)$_2$ > SO(*p*-MeC_6H_4)$_2$ > $SOPh_2$ > $SO(Bz)_2$ > SO(*p*-ClC_6H_4)$_2$ > SO(*sec*-Bu)$_2$ > SO(*i*-Pr)$_2$ and is strongly affected by the nature of the substituents bonded to the sulfur atom.

QALE Analysis. Giering and Prock[3a−g] have suggested the equations and the protocol to perform a quantitative analysis (QALE) of the steric and electronic effects of ligands. A large body of kinetic, thermodynamic, NMR, and IR data and other physicochemical properties that depend on the stereoelectronic characteristics of the ligands have been analyzed successfully with QALE. Very recently these authors have collected all the available material (i.e., sets of data, protocol for the analysis, program package, parameters of the ligands, leading references, etc.) in a flexible tool such as a Web site, subjecting each set of data to a QALE analysis with commentary on how each analysis is done and how successful it is.[5] Essentially, the protocol implies a combined method, based on the use of data obtained from graphical analysis to control the results of the regression analysis.

We took advantage of an essential tenet of QALE which allows the stereoelectronic parameters to be transferred from AZ_3 (A = P, phosphines) to AZ_2 (A = SO, sulfoxides), as done before by Giering et al. for thioethers.[6] However, we were unable with this method to confer suitable steric or electronic parameters to $SO(Bz)_2$, $SO(CH_2)_4$, and SOMe(*p*-BrC_6H_4). Therefore, the parameter χ in Table 1 describes the σ electron donor capacity of the ligands (a small χ value is associated with a good σ donation),[7] θ is Tolman's cone angle,[8] which measures the size of the ligand, and E_{ar} is a secondary electronic effect of unknown origin which is generally associated with the number of pendent aryl groups,[9] even if it is not limited to it. The response of the kinetic data to χ and E_{ar} is assumed to be linear over the entire set of ligands, while the response to the steric parameter θ is not linear for the possibility of the onset of a steric threshold. A steric threshold marks the point below or above which no steric effects are evident.[10]

We start the interpretation of the kinetic data by analyzing the plot of log k_2 versus χ in Figure 3. The line determined

(5) http://www.bu.edu/qale/.
(6) Fernandez, A. L.; Prock, A.; Giering, W. P. *Organometallics* **1996**, *15*, 2784−2789 and references therein.
(7) Bartik, T.; Himmler, T.; Schulte, H.; Seevogel, K. J. *J. Organomet. Chem.* **1984**, *272*, 29−41.
(8) Tolman, C. A. *Chem. Rev.* **1977**, *77*, 313−348.
(9) Wilson, M. R.; Woska, D. C.; Prock, A.; Giering, W. P. *Organometallics* **1993**, *12*, 1742−1752.
(10) Liu, H.-Y.; Eriks, K.; Prock, A.; Giering, W. P. *Organometallics* **1990**, *9*, 1758−1766.

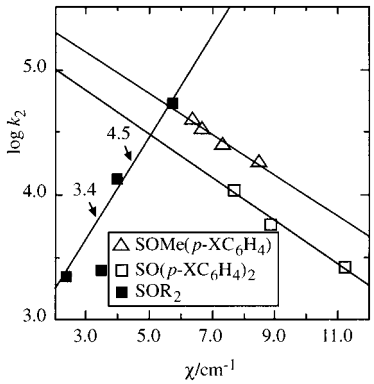

Figure 3. Graphical analysis of log $k_{2(obsd)}$ for the fluxional motion promoted by sulfoxides in complex **1** (see the text). The datum for SO(*sec*-Bu)$_2$ is considered an outlier. The intersections of the lines for SOMe(*p*-XC_6H_4) and SO(*p*-XC_6H_4)$_2$ with that for SOR_2 occur at $\chi = 5.7$ and $\chi = 4.9$, rather than at $\chi = 4.5$ and $\chi = 3.4$, respectively.

by the data for SO(*p*-XC_6H_4)$_2$ has a slope of -0.17 ± 0.02. Since the SO(*p*-XC_6H_4)$_2$ ligands are isosteric and possess the same number of aryl groups, the slope of this plot affords an estimate of the coefficient of χ for the full set of data in the QALE equation. In practice, from the pattern of behavior of a subset of ligands having θ and E_{ar} constants, we get fast information on the sensitivity of the system to the electron release of substituents on sulfur. The line determined by the data for SOMe(*p*-XC_6H_4) appears to be parallel to the line for SO(*p*-XC_6H_4)$_2$. The data for three of the SOR_2 ligands fit a reasonably good straight line, while the datum for SO(*sec*-Bu)$_2$ appears to be an outlier.[11] Since the latter line, in contrast to those for the SOMe(*p*-XC_6H_4) and SO(*p*-XC_6H_4)$_2$ ligands, has a positive slope, we can conclude that there is a dominant and inhibitory steric effect associated with the SOR_2 ligands. In the absence of an aryl effect, the two parallel lines would have intersected the SOR_2 line at points 4.5 and 3.4. The magnitude of the deviation observed is a measure of the E_{ar} effect. The latter enhances the reactivity of SO(*p*-XC_6H_4)$_2$ as compared to those of SOMe(*p*-XC_6H_4) and the SOR_2 ligands. Plots of log k_2 versus the number of aryl groups (i) in the series $SOPh_iMe_{2-i}$ are reasonably linear (see Supporting Information Figure S2), suggesting the absence of a steric threshold. Application of the steric threshold program supports this conclusion.

Since there is no evidence for a steric threshold, and only steric (θ) and electronic ($\sigma + E_{ar}$) effects were found to be operative, the appropriate equation to analyze the data is

$$\log k_2 = \omega + \alpha(\chi) + \beta(\theta) + \gamma(E_{ar}) \qquad (3)$$

where α, β, and γ are regression coefficients that measure the relative importance of electronic, steric, and E_{ar} factors in the process. All the kinetic data in Table 1 for which we have parameters, except that for SO(*sec*-Bu)$_2$ considered an outlier, were analyzed with the above equation. The results obtained using the SCIENTIST program are listed in Table 2. As a measure of the goodness of fit, we used the value of r^2, which measures the fraction of the total variance accounted for by the model. When dealing with a multiplicity of possible models, a more appropriate index of the goodness of fit is the MSC (model selection criterion) value.[12] The most appropriate model will be that with the largest MSC. A supplementary statistical criterion is given by the value of $r^2 = 0.995$ for the linear plot of log $k_{2(calcd)}$ vs log $k_{2(obsd)}$, where log $k_{2(calcd)}$ is obtained by introducing the calculated coefficients in eq 3. Another appropriate index of the goodness of fit is given by the correspondence between the value of α (-0.17 ± 0.03) obtained from full regression analysis and that (-0.17 ± 0.02) obtained from the plots of log k_2 vs χ for the isosteric ligands SO(*p*-XC_6H_4)$_2$ and SOMe(*p*-XC_6H_4), characterized by the values of the θ and E_{ar} constants. Attempts to apply the sum of Taft's σ^* constants as electronic parameters, or the Calligaris circular cone apertures[13] as a measure of the steric requirement of the ligands, led to a poorer correlation than with χ and θ.

The results of the QALE analysis can now be displayed as electronic, steric, and E_{ar} profiles (Figure 4). The electronic profile (Figure 4A) indicates that the rate of fluxional motion of dmphen in **1** is enhanced as the sulfoxides become better electron donors (smaller χ), and can be constructed by subtracting the contributions of all the terms of the regression equation, except that of the variable of interest, i.e., $\alpha(\chi)$, from the experimental data, according to the equation

$$\log k_2(\chi) = \log k_{2(obsd)} - (\beta(\theta) + \gamma(E_{ar}) + \omega) \qquad (4)$$

Likewise, the steric profile (Figure 4B) and the E_{ar} profile (Figure 4C) can be constructed using similar equations. Figure 4B indicates that the rate of dmphen flipping diminishes as the size of the sulfoxide increases, and Figure 4C indicates that the presence of an aryl group enhances the reactivity of the sulfoxide and, thereby, the rate of reaction. Parts A−C of Figure 4 are presented with the same absolute scale to give a visual comparison of the relative importance of the three parameters. However, another useful way to display the extent to which a parameter affects a property is to calculate the percentage contribution of that parameter, using the regression coefficients derived from eq 3 and defining the maximum range of variation of the parameters ($\Delta\chi = 26$ cm^{-1}; $\Delta\theta = 60°$; $\Delta E_{ar} = 2$),[5] according to the equation

$$\%\chi = 100(|\alpha|\Delta\chi)/[(|\alpha|\Delta\chi) + (|\beta|\Delta\theta) + (|\gamma|\Delta E_{ar})] \qquad (5)$$

Therefore, log k_2 exhibits a 45% electronic contribution, a 45% steric contribution, and only a 10% E_{ar} contribution.

The kinetic data (log $k_{2'}$) for the reaction of sulfoxides with **2** were analyzed in the same manner. The results are

(11) The steric and electronic properties of SO(*sec*-Bu)$_2$ should resemble those of SO(*i*-Pr)$_2$ rather than those of SO(*n*-Bu)$_2$. As a matter of fact Bartik's value of χ for P(*sec*-Bu)$_3$ (on which the χ value of SO(*sec*-Bu)$_2$ is based) is closer to that of P(*n*-Bu$_3$) than it is to that of P(*i*-Pr)$_3$. The datum for SO(*sec*-Bu)$_2$ fits the graphical analysis when it is assigned the same χ value as that for SO(*i*-Pr)$_2$.

(12) When comparing two models with different numbers of parameters, this criterion not only places a burden on the model with more parameters to have a better coefficient of determination, but also quantifies how much better it must be for the model to be deemed more appropriate.

(13) Calligaris, M.; Faleschini, P.; Todone, F.; Alessio, E.; Geremia, S. *J. Chem. Soc., Dalton Trans.* **1995**, 1653−1661.

Table 2. Selected Coefficients Derived from QALE Analysis on the Second-Order Rate Constants (k_2) of Some Reactions on Platinum(II) Complexes

complex	reagent	type of reaction	n^a	α^b	β^c	γ	ω	r^2	MSC^d
[Pt(Me)(dmphen)(PPh$_3$)]$^+$ ^{e}	SOR_1R_2	fluxionality	12	-0.17 ± 0.03	-0.076 ± 0.006	0.49 ± 0.1	11.9 ± 0.7	0.952	2.37
% contribution of params				45	45	10			
[Pt(Me)(phen)(SOMe$_2$)]$^+$ ^{e}	SOR_1R_2	substitution	7	-0.34 ± 0.03	-0.052 ± 0.004	0.61 ± 0.08	3.9 ± 0.4	0.99	3.55
% contribution of params				67	24	9			
[PtPh$_2$(CO)(5-Aq)]^f	$PR_1R_2R_3$	substitution	13	-0.07 ± 0.03	-0.099 ± 0.005	0.3 ± 0.1	14.6 ± 0.8	0.983	3.62
% contribution of params				22	66	12			
[Pt(NNC)Cl]^g	$PR_1R_2R_3$	substitution	14	-0.134 ± 0.02	-0.075 ± 0.005	0.4 ± 0.1	13.8 ± 0.8	0.962	2.70
% contribution of params				38	48	14			

^{a} Number of data points. ^{b} Centimeters. ^{c} Inverse degrees. ^{d} See the text and ref 12. ^{e} This work. ^{f} From ref 14, leaving group = 5-aminoquinoline (5-Aq). ^{g} From ref 15, leaving group = chloride (N−N−CH = 6-(1-methylbenzyl)-2,2′-bipyridine).

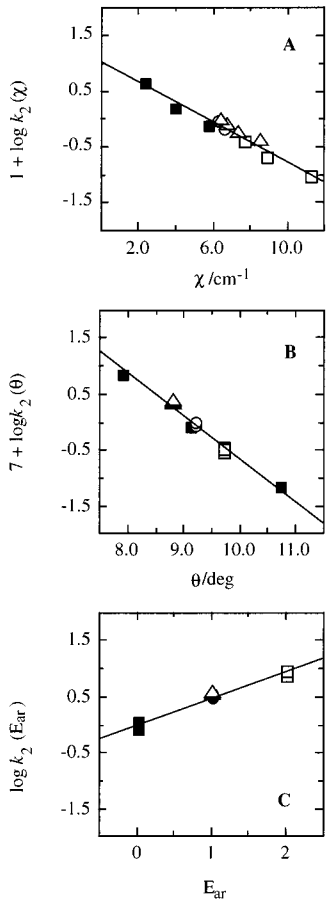

Figure 4. Electronic profile (A), steric profile (B), and E_{ar} plot (C) for sulfoxides acting as catalysts on the fluxional motion of dmphen in complex **1**. Filled squares refer to dialkyl sulfoxides, open circles to SOEt(Ph) and SOPr(Ph), open squares to SO(p-XC_6H_4)$_2$, and open triangles to SOMe(p-XC_6H_4).

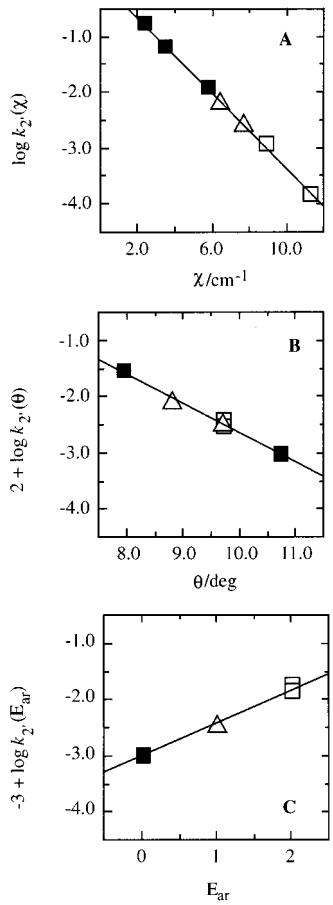

Figure 5. Electronic profile (A), steric profile (B) and E_{ar} plot (C) for sulfoxides acting as entering groups in the nucleophilic substitution reaction of $SOMe_2$ from complex **2**. Filled squares refer to dialkyl sulfoxides, open squares to SO(p-XC_6H_4)$_2$, and open triangles to SOMe(p-XC_6H_4).

listed in Table 2 and are illustrated in Figure 5. We can see that the signs of the coefficients of χ and θ of both processes (fluxionality on **1** and substitution on **2**) are characteristic of entering-ligand-dependent substitution reactions. Thus, the negative sign of the α coefficient indicates that the transition state is electron demanding relative to the ground state. The negative sign of the β coefficient indicates that the increasing steric requirement of the ligand impedes the reaction. The relative magnitudes of the coefficients give insight into the nature of the transition states of these reactions. By comparing the data in Table 2, we can see that the contribution of E_{ar} is small if not negligible for both processes. The steric and electronic contributions are of about equal importance for the fluxional process in **1**, while the electronic effect is prevalent (67%) with respect to the steric effect (24%) in the substitution reactions in complex **2**. The sensitivity to electronic effects is a measure of the extent of metal−ligand bond making in the transition state. Thus, there is a greater platinum−sulfur interaction in the transition state of **2** than in the transition state of **1**. The QALE analysis shows that the five-coordinate transition state of **2** is more associative in nature than the transition state of **1**. These conclusions are in line with the structural features of the two complexes under investigation. Other examples of associative substitution reactions on platinum complexes for which a complete

QALE analysis has been performed refer to the use of phosphines as reagents in the substitution of 5-aminoquinoline (5-Aq) from $[PtPh_2(CO)(5\text{-Aq})]$[14] and of chloride from the cyclometalated complex [Pt(N−N−C)Cl] (N−N−CH = 6-(1-methylbenzyl)-2,2′-bipyridine).[15] The results are summarized in Table 2. A survey of the literature data suggests that a number of other entering-ligand-dependent substitution reactions have been analyzed with eq 3, including the heat of reaction of *trans*-$[Pt(Me)L_2(THF)]^+$ with phosphines,[16] the displacement of acetone from $[\eta^5\text{-}(C_5R_5)(CO)Fe(Ac)(COMe)]^+$ with thioethers,[6] etc.

The Mechanism. The fluxional motion of dmphen in $[Pt(Me)(dmphen)(PPh_3)]^+$, catalyzed by sulfoxides, exhibits a pattern strictly similar to that of bimolecular nucleophilic substitution reactions.[17] Akin to the displacement of a ligand in a square-planar complex, the rate-determining step is the attack of a nucleophile to the metal, which takes place with a low enthalpy of activation and a largely negative entropy of activation ($\Delta H^{\ddagger} = 24.2 \pm 0.5$ kJ mol^{-1} and $\Delta S^{\ddagger} = -70 \pm 2$ J K^{-1} mol^{-1}, in the presence of dmso-d_6 8.66 m*m*). The free energy for the catalyzed process ($\Delta G^{\ddagger} = 45$ kJ mol^{-1}) is at least 20 kJ mol^{-1} lower than that for the dissociative uncatalyzed flipping of dmphen in **1** (66.5 kJ mol^{-1})[1] (see Supporting Information Figure S1). The kinetics clearly indicate that a key step in the fluxional mechanism of **1** is the formation of a five-coordinate intermediate upon sulfoxide coordination. Therefore, in addressing the question of how the fluxional motion of the dinitrogen ligand occurs, besides the obvious traditional consecutive displacement mechanism, we must take into account the possibility of intramolecular rearrangements from a five-coordinate intermediate, such as some form of Berry pseudorotation or a turnstile mechanism (Scheme 2). No distinction can be made among the three possible reaction pathways on the basis of the rate law or the structural effects observed. The difficulty of differentiating between these mechanisms, using kinetic data alone, has been known for many years. Anderson and Cross,[18] in an excellent review paper on the isomerization mechanism of square-planar complexes, have pointed out that different authors have used the same evidence to support radically different opinions. We avoid adding a new case in contest, being aware that the one-step transfer of the sulfoxide to the substrate leads the five-coordinate intermediate to occupy a point of high energy along the energy profile, and any discussion on the nature of the subsequent minima along this profile risks becoming semantic in nature. However, it is useful to comment briefly on the various alternatives.

Pseudorotation of five-coordinated species is difficult to reconcile with the highly stereospecific nature of substitutions

Scheme 2. Sequence of Berry Pseudorotations (Left Side) and Turnstile Intramolecular Rearrangements (Right Side) of a Five-Coordinate Intermediate, Leading to the Exchange of Coordination Sites of the Pt−N Bonds in **1**

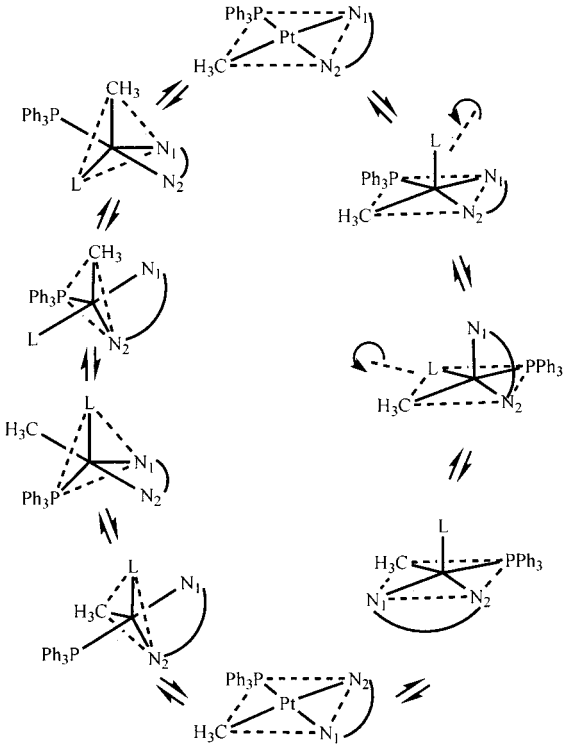

on Pt(II). Its operation here could be favored by the fact that all the potential rearrangements of the trigonal bipyramids (left side of Scheme 2) could involve the participation of the N−N ligand in an axial−equatorial coordination. This could appear to be an easy situation for a rigid ligand with a small bite angle such as dmphen. The same reasoning applies for the sequence of turnstile rearrangements necessary to originate a site exchange for the two nitrogen atoms of the dmphen ligand (right side of Scheme 2). Interestingly, the best documented example of operation of such a mechanism[2b] requires a square-pyramidal coordination, since the ligands used make the trigonal-bipyramidal coordination very strained.

The most likely consecutive displacement mechanism that can be envisaged consists of a sequence of nucleophilic substitution reactions, which take place with complete retention of configuration (Scheme 3). The process features a catalyzed geometrical isomerization, many examples of which can be found in the literature.[18−23] The mechanism involves the opening of one arm of the bidentate N−N ligand upon nucleophilic attack by the ligand L, and the interconversion of two η^1-coordinated complexes via formation of a common five-coordinate chelated intermediate. The latter requires the participation of the phenanthroline as an equatorial ligand, in the trigonal $Ph_3P-Pt\{\eta^2\text{-}(N1-N2)\}$ moiety,

(14) Romeo, R.; Arena, G.; Monsù Scolaro, L. *Inorg. Chem.* **1992**, *31*, 4879−4884.
(15) Romeo, R.; Plutino, M. R.; Monsù Scolaro, L.; Stoccoro, S. *Inorg. Chim. Acta* **1997**, *265*, 225−233.
(16) Manzer, L. E.; Tolman, C. A. *J. Am. Chem. Soc.* **1975**, *97*, 1955−1956.
(17) (a) Tobe, M. L.; Burgess, J. *Inorganic Reaction Mechanisms*; Addison-Wesley Longman: Essex, England, 1999. (b) Wilkins, R. G. *Kinetics and Mechanisms of Reactions of Transition Metal Complexes*; VCH: Weinheim, Germany, 1991. (c) Basolo, F. *Coord. Chem. Rev.* **1996**, *154*, 151−161.
(18) Anderson, G. K.; Cross, R. J. *Chem. Soc. Rev.* **1980**, *9*, 185−215.
(19) Romeo, R. *Comments Inorg. Chem.* **1990**, *11*, 21−57.
(20) Cattalini, L.; Martelli, M. *J. Am. Chem. Soc.* **1969**, *91*, 312−316.
(21) Roulet, R.; Barbey, C. *Helv. Chim. Acta* **1973**, *56*, 2179−2186.
(22) Annibale, G.; Bonivento, M.; Canovese, L.; Cattalini, L.; Michelon, G.; Tobe, M. L. *Inorg. Chem.* **1985**, *24*, 797−800.
(23) Favez, R.; Roulet, R.; Pinkerton, A. A.; Schwatzenbach, D. *Inorg. Chem.* **1980**, *19*, 1356−1365.

Scheme 3. Sequence of Stereospecific Ring-Opening Reaction Steps, Leading to the Exchange of Coordination Sites of the Pt−N Bonds in **1**, through a Chelated Five-Coordinated Intermediate

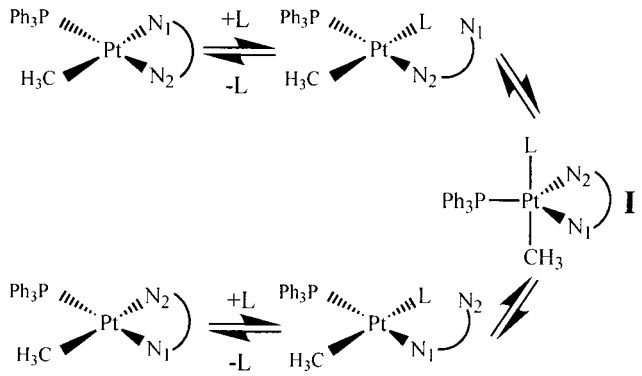

with the two nitrogen donors being equivalent with respect to the coordinated sulfoxide. This coordinating geometry apparently looks uneasy for a rigid ligand with a small bite angle. In fact, a number of X-ray structural studies of five-coordinate trigonal-bipyramidal platinum(II) complexes have shown that dmphen lies in the trigonal plane, forming a flat unconstrained five-membered ring,[24] even if a rare case for axial−equatorial N−N coordination has been reported.[25] Panunzi and Natile[26] have discussed at length the reasons why a chelate ring, either flat or puckered, produced by a bidentate dinitrogen ligand, occupies two equatorial sites in a five-coordinate trigonal-bipyramidal platinum(II) complex and have shown evidence of how an increase of the bite angle destabilizes the trigonal bipyramid, which shifts to a square-planar geometry by chelate ring opening.

If one does not object to the equatorial chelate, which we do not, the displacement mechanism in Scheme 3 becomes the most reasonable interpretation for the following reasons: (i) it involves only stereospecific steps, and (ii) it accounts for the lability of the nitrogen−platinum bond. The weakening of the Pt−N1 and Pt−N2 bonds, under the *trans* influence of the strong σ donors methyl and phosphine groups, appears to be a factor of overwhelming importance in dictating the dynamic motion of dmphen. Easy Pt−N bond dissociation facilitates the ring opening either in the original square-planar complex (spontaneous fluxional motion of the phenanthroline in **1**) or in a bipyramidal trigonal coordinative environment (catalyzed flipping of dmphen). Accordingly, the addition of external ligands to **1** must be carried out with care to avoid dmphen displacement, which, however, inevitably takes place with traces of the most nucleophilic ligands, such as phosphines or halide ions. Compounds similar to **1**, where PPh_3 has been substituted by less efficient *trans*-activating groups (amine, pyridine, and thiourea) behave as stereochemically rigid N,N-chelated complexes.[1] Likewise, a static structure characterizes complexes containing 1,10-phenanthroline such as **2**, and the removal of the chelated ligand hardly occurs, even by adding an excess of strong nucleophiles. A further impetus to ring opening comes from the release of steric congestion in forming a complex in which dmphen is η^1-coordinated. In conclusion, although the kinetics do not prove or disprove the operation of alternative mechanisms, such as those depicted in Scheme 2, where N−N remains η^2-coordinated, a consecutive stepwise displacement mechanism is to be preferred. This can be inferred by the strict correlation between the facility of Pt−N bond breaking and the fluxional motion of the dinitrogen ligand and the well-known preference of platinum(II) complexes to undergo stereospecific substitutions.

Within this mechanistic framework, it would be of interest to extend the study to the fluxionality of **1** promoted by other families of ligands such as thioethers or amines. However, a fascinating aspect of this system appears to be the uncatalyzed intrinsic fluxionality of $[Pt(Me)(dmphen)(L)]^+$ cationic complexes, which involves a dissociative mechanism and is connected to the capacity of the ligand L in promoting Pt−N bond dissociation. A detailed kinetic study is underway on complexes in which L represents an extended series of phosphines, with the aim of ascertaining the relative importance of steric and electronic factors of "spectator" ligands in governing the fluxionality of the substrates.

Experimental Section

Synthesis of the Complexes. The complex $[Pt(Me)(dmphen)(PPh_3)]PF_6$ (**1**) was prepared following the published procedure.[1] **[Pt(Me)(phen)(SOMe$_2$)]TFPB (2)** (TFPB = $B[3,5\text{-}(CF_3)_2C_6H_3]_4$) was obtained by ion exchange, by adding a stoichiometric amount of NaTFPB[27] to a dichloromethane solution of $[Pt(Me)(phen)(SOMe_2)]PF_6$.[28] The salt $NaPF_6$ that separated out as a solid from the solution was filtered off, and the complex was obtained by evaporation of the residual solvent. ^{1}H NMR ($CDCl_3$, T = 298 K): δ 10.09 (dd, $^3J_{PtH}$ = 18.7 Hz, $^3J_{HH}$ = 5.5 Hz, $^4J_{HH}$ = 1.1 Hz, 1H, H_9), 9.04 (dd, $^3J_{PtH}$ = 46.2 Hz, $^3J_{HH}$ = 5.5 Hz, $^4J_{HH}$ = 1.1 Hz, 1H, H_2), 8.62 (d, $^3J_{HH}$ = 8.2 Hz, 1H, H_7), 8.58 (d, $^3J_{HH}$ = 8.2 Hz, 1H, H_4), 8.01 (dd, $^3J_{HH}$ = 8.2, 5.5 Hz, 1H, H_8), 7.99 (AB system, $^3J_{HH}$ = 8.8 Hz, 1H, H_5), 7.93 (AB system, $^3J_{HH}$ = 8.8 Hz, 1H, H_6), 7.89 (dd, $^3J_{HH}$ = 8.2, 5.5 Hz, 1H, H_3), 7.71 (s, br, 8H, $H_{o,o'}$), 7.48 (s, br, 4H, H_p), 3.50 (s, $^3J_{PtH}$ = 36.8 Hz, 6H, S-CH_3), 0.90 (s, $^2J_{PtH}$ = 72.0 Hz, 3H, Pt-CH_3). Anal. Calcd for $PtBC_{47}H_{29}F_{24}N_2OS$: C, 42.4; H, 2.2; N, 2.1. Found: C, 42.4; H, 2.4; N, 2.1.

General Procedures and Chemicals. Sulfoxides and sulfides were purchased from Lancaster or Aldrich Chemical Co. The crystalline sulfoxide $SOPh_2$ was dried by being allowed to stand for many hours under vacuum over P_4O_{10}. Pure $SO(sec\text{-}Bu)_2$, SOEt(Ph), $SOMe(p\text{-}ClC_6H_4)$, and $SOMe(p\text{-}MeOC_6H_4)$ were obtained by oxidation of the corresponding sulfides with 3-chloroperoxybenzoic

(24) (a) Fanizzi, F. P.; Intini, F. P.; Maresca, L.; Natile, G.; Lanfranchi, M.; Tiripicchio, A. *J. Chem. Soc., Dalton Trans.* **1991**, 1007−1015. (b) Albano, V. G.; Ferrara, M. L.; Monari, M.; Panunzi, A.; Ruffo, F. *Inorg. Chim. Acta* **1999**, *285*, 70−75. (c) De Felice, V.; Ferrara, M. L.; Giordano, F.; Ruffo, F. *Gazz. Chim. Ital.* **1994**, *124*, 117−119. (d) Giordano, F.; Ruffo, F.; Saporito, A.; Panunzi, A. *Inorg. Chim. Acta* **1997**, *264*, 231−237. (e) Fanizzi, F. P.; Natile, G.; Lanfranchi, M.; Tiripicchio, A.; Pacchioni, G. *Inorg. Chim. Acta* **1998**, *275*−*276*, 500−509. (f) Albano, V. G.; Castellari, C.; Monari, M.; De Felice, V.; Panunzi, A.; Ruffo, F. *Organometallics* **1996**, *15*, 4012−4019. (g) Albano, V. G.; Castellari, C.; Monari, M.; De Felice, V.; Panunzi, A.; Ruffo, F. *Organometallics* **1992**, *11*, 3665−3669.

(25) Albano, V. G.; Monari, M.; Orabona, I.; Ruffo, F.; Vitagliano, A. *Inorg. Chim. Acta* **1997**, *265*, 35−46.

(26) (a) Albano, V. G.; Natile, G.; Panunzi, A. *Coord. Chem. Rev.* **1994**, *133*, 67−114. (b) Maresca L.; Natile, G. *Comments Inorg. Chem.* **1993**, *14*, 349−366.

(27) Brookhart, M.; Grant, B.; Volpe, A. F. *Organometallics* **1992**, *11*, 3920−3922.

(28) Romeo, R.; Monsù Scolaro, L.; Nastasi, N.; Arena, G. *Inorg. Chem.* **1996**, *35*, 5087−5096.

acid (Aldrich).[29] The compounds were obtained as pure products after silica gel chromatography with petroleum ether and ethyl acetate (9:1, v/v), and their purity was checked by IR and ^{1}H NMR measurements. All the other sulfoxides were used as received from Lancaster or Aldrich. Solvents (from Aldrich) used in the synthetic procedures were distilled under nitrogen from the appropriate drying agents (diethyl ether from sodium benzophenone ketyl, dichloromethane from barium oxide, and dimethyl sulfoxide, at low pressure, from CaH_2, after preliminary filtration through an alumina column) and then stored in N_2-filled flasks over activated 4 Å molecular sieves. Chloroform-*d* (+99.96% D, Cambridge Isotope Laboratories) was dried by being allowed to stand for many days over CaH_2, distilled under nitrogen over activated magnesium sulfate and sodium carbonate, and then stored over activated 4 Å molecular sieves. K_2PtCl_4 (Strem) was purified by dissolving it in water and filtering. Commercial reagent grade chemicals dmphen and phen were used without further purification. Triphenylphosphine (Strem) was crystallized from ethanol by dissolving it in the hot solvent, filtering, and cooling the filtrate to 0 °C.

Instrumentation. Infrared spectra were recorded as Nujol mulls or neat using CsI disks on a Perkin-Elmer FT-IR model 1730 spectrophotometer. ^{1}H and ^{31}P{^{1}H} NMR spectra were obtained in $CDCl_3$ solution on a Bruker AMX R-300 spectrometer equipped with a broad-band probe operating at 300.13 and 121.49 MHz, respectively. ^{1}H chemical shifts were measured relative to the residual solvent peak and are reported in δ units downfield from Me_4Si. ^{31}P chemical shifts, in parts per million, are given relative to that of external 85% phosphoric acid. The temperature within the probe was checked using the methanol or ethylene glycol method.[30]

Kinetics. The rates of the fluxional motion of dmphen in complex **1** and of sulfoxide exchange and substitution in complex **2** were obtained by various dynamic ^{1}H NMR techniques.

Line-Shape Analysis. In a typical set of ligand-concentration-dependent experiments, carried out at constant temperature (298 K), approximately 10 mg of complex **1** was dissolved in 0.5 mL of dried $CDCl_3$, and the initial NMR spectrum was recorded. The subsequent NMR spectra were taken after the addition of the appropriate amount of sulfoxide. All concentrations of the ligand are expressed in moles per kilogram of solvent (m = mol kg^{-1}). The methyl protons of the substituted phenanthroline were used for the line-shape analysis. The spectral simulation was performed using the computer program gNMR 4.0.[31] A satisfactory fit between the simulated and observed spectra was judged both by visual comparison and by a least-squares fit. The variable-temperature experiments were carried out by recording the spectrum of a solution, prepared as described above, over a proper temperature range. The activation parameters $\Delta G^{\ddagger}$, $\Delta H^{\ddagger}$, and $\Delta S^{\ddagger}$ were derived from linear regression analysis of the Eyring plot.

Isotopic Exchange. The kinetic study of $SOMe_2$ exchange on **2** was performed by adding with a microsyringe a known volume of dimethyl sulfoxide-d_6 on a prethermostated solution of weighted complex in $CDCl_3$. At least a 5-fold excess of dmso-d_6 over the complex was ensured in any run. The isotopic exchange was followed by monitoring the increase in intensity of the proton NMR signal of free nondeuterated $SOMe_2$ at δ 2.60 ppm and the matching decrease of the signal of the sulfoxide coordinated to the metal. The spectra were recorded at appropriate intervals of time. The mole fraction $F = [SOMe_2]_f/([SOMe_2]_f + [SOMe_2]_b)$ of the free dimethyl sulfoxide was obtained by integration of the signals, and the first-order rate constants k_{exch} (s^{-1}) for the exchange of the label were obtained from a nonlinear least-squares fit of the experimental data to $F = c_1 + c_2 \exp(-k_{exch}t)$, with c_1, c_2, and k_{exch} as the parameters to be optimized. A similar analysis can be performed by using the mole fraction of the bound dimethyl sulfoxide. From the McKay equation, $R_{exch} = k_{exch}ab(a + b)^{-1}$ (where R_{exch} is the rate of the exchange process, a the concentration of the complex, and b the concentration of free sulfoxide), the pseudo-first-order rate constants, $k_{obsd} = R_{exch}/a$, were calculated.

Sulfoxide Substitutions. The kinetic study of ligand substitution on **2** was carried out in $CDCl_3$ at 298 K by following the same procedure described for the isotopic exchange. After addition of the appropriate amount of the proper sulfoxide, the ^{1}H NMR spectra were recorded at various time intervals. The signals of released and bound $SOMe_2$ were monitored, and the first-order rate constants k_{obsd} (s^{-1}) were calculated from a nonlinear least-squares fit of the experimental data to $F = c_1 + c_2 \exp(-k_{obsd}t)$, where F is the mole fraction of one of the reagents, calculated as described above. In some reactions ($SO(sec\text{-}Bu)_2$, $SO(p\text{-}MeC_6H_4)_2$, $SOPh_2$, and $SO(p\text{-}ClC_6H_4)_2$), it was necessary to account for the possible reentry of free $SOMe_2$ into the coordination sphere of the metal, and therefore the rate data were calculated by using the SCIENTIST software package[32] and the differential equation $-d[A]/dt = k_f[A][Y] - k_r[B][SOMe_2]$, where [A] and [B] are the concentrations of complex **2** and of the final product, respectively, while [Y] represents the concentration of the added sulfoxide. k_f and k_r (m^{-1} s^{-1}) are the second-order rate constants for substitution of $SOMe_2$ from **2** and for the reverse reaction, respectively.

Acknowledgment. We thank the Ministero dell'Istruzione dell'Università e della Ricerca (MIUR), Programmi di Ricerca Scientifica di Rilevante Interesse Nazionale, Cofinanziamento 2000−2002, the Università degli Studi di Messina, and CNR for funding this work. We also gratefully thank Prof. W. P. Giering for helpful discussions.

Supporting Information Available: Tables S1 and S3 giving primary kinetic data (pseudo-first-order rate constants (k_{obsd}/s^{-1}) for the fluxional motion in **1** and for nucleophilic substitution on compound **2**, as a function of [SOR(R′)]), Table S2 and Figure S1 for the temperature dependence of the uncatalyzed and catalyzed flipping in **1**, and Figure S2 illustrating the dependence of the fluxional rate of compound **1** upon the number of pendent aryl groups in SOR(R′). This material is available free of charge via the Internet at http://pubs.acs.org.

IC011206J

(29) Aversa, M. C.; Barattucci, A.; Bonaccorsi, P.; Giannetto, P.; Jones, D. N. *J. Org. Chem.* **1997**, *62*, 4376−4384 and references therein.
(30) (a) Van Geet, A. L. *Anal. Chem.* **1968**, *40*, 2227−2229. (b) Van Geet, A. L. *Anal. Chem.* **1970**, *42*, 679−680.
(31) gNMR 4.0, Cherwell Science, Oxford.
(32) SCIENTIST, Micro Math Scientific Software, Salt Lake City, UT.